RESEARCH ARTICLE **ISSN 2738-9898 (Print) ISSN 2738-9901 (Online)**

PSO-based PID controller for frequency control of two area interconnected power system

Sandip Dumre[1]* and Purna Bahadur Pun[2]

[1]Department of Electrical Engineering, Institute of Engineering, Pashchimanchal Campus, Tribhuvan University,Pokhara, Nepal

[2]School of Engineering, Faculty of Science and Technology, Pokhara University, Pokhara , Nepal

* Author to whom correspondence should be addressed; E-Mail: *sandeep.dumre136@gmail.com*

Received: 10 December, 2024; Received in revised form: 31 December, 2024; Accepted: 14 January, 2025; Published: 31January, 2025

Abstract

This paper presents an analysis of the dynamic performance of frequency control in a two-area interconnected power system using a Particle Swarm Optimization (PSO)-based PID controller. Maintaining stable system frequency within specified limits is crucial for the efficient operation of power system equipment. The proposed power system model comprises synchronous generators, loads in two distinct areas, and a photovoltaic (PV) system in Area-1. The system is modeled in MATLAB Simulink to analyze the impact of load variations and PV generation on system frequency. PSO, an evolutionary optimization technique, is employed to determine the optimal PID controller gains, minimizing frequency deviations. Three load increase scenarios in the two-area system were considered to evaluate the performance of the proposed controller. The results demonstrate the effectiveness of the PSO-based PID controller in mitigating frequency deviations, enhancing system stability and reliability. This study provides valuable insights into automatic optimal tuning of PID controllers in two-area systems, contributing to improved stability and operational reliability in power systems.

Keywords

Two Area System, Frequency Control, Tie-line, Proportional-Integral-Derivative (PID) controller, Particle Swarm Optimization (PSO)

1. Introduction

Power systems are designed to provide consistent and reliable electricity by managing complex networks of generation, transmission, and distribution infrastructure. The stability of a power system is essential for ensuring reliable service to consumers. A key aspect of this stability lies in maintaining balanced voltage and frequency levels, which can fluctuate due to changes in load demand. The control challenges in power systems can be categorized into two independent problems: frequency control, primarily governed by active power, and voltage control, which depends on reactive power. Load Frequency Control (LFC) is a critical mechanism responsible for maintaining frequency stability by balancing the active power between generation and load.

The frequency stability of a power system is influenced by various factors, including system inertia, droop, and turbine/governor dynamics. Inertia, provided by the rotational mass of

synchronous generators and induction motors, plays a vital role in suppressing frequency deviations and slowing frequency dynamics. This response enables the system to withstand disturbances such as load changes, power plant outages, and grid faults. Frequency deviations, caused by an imbalance in active power, are immediately reflected across the interconnected system, making LFC indispensable for stability and reliability. Also, the integration of renewable energy sources (RESs) introduces new challenges to power networks. Renewable energy systems, such as photovoltaic (PV) arrays, lack rotational inertia, resulting in a significant reduction in the overall system inertia. This leads to increased frequency deviations and diminished response times during disturbances. Furthermore, the variability in renewable power generation due to factors like temperature, irradiance, and changing load demands complicates the frequency control mechanisms of the system. To address these challenges, various control strategies have been developed for LFC. Among these, proportional-integral-derivative (PID) controllers remain a popular choice due to their simple structure, robustness, and adaptability to system parameter uncertainties. PID controllers effectively minimize the deviation between the desired and actual frequency levels, providing stability and faster response. Advanced control methods, including fuzzy logic, artificial neural networks, and distributed model predictive controllers, have also been explored to enhance system performance. Additionally, optimization techniques such as the Particle Swarm Optimization (PSO) algorithm have proven effective in fine-tuning controller parameters to achieve improved accuracy and dynamic response.

This paper focuses on the principles and mechanisms of LFC, emphasizing its importance in power systems, particularly in modern grids with a high penetration of renewable energy sources. The study highlights the role of inertia, the challenges posed by renewable integration, and the effectiveness of PID controllers and optimization algorithms in maintaining frequency stability. The research paper [1] examines the Load Frequency Control (LFC) of the Integrated Nepal Power System (INPS), focusing on the management of frequency and power output in an interconnected power network. It models the system using two areas: Area-1 representing INPS and Area-2 representing the Indian Power System, highlighting the challenges and strategies involved in maintaining system stability across the interconnected grids.

Paper [2] analyzes Load Frequency Control (LFC) in a multi-source power system with two interconnected areas, focusing on maintaining steady-state frequency and tie-line interchange errors within acceptable limits. Due to fluctuations in Renewable Energy Sources (REs), power imbalances and frequency deviations may occur. A Genetic Algorithm (GA)-based PID controller is proposed, incorporating an Energy Storage System (ESS) for auxiliary regulation. Time-domain simulations, conducted under various scenarios, show the effectiveness of the control scheme. Sensitivity analysis reveals that the designed controllers are robust, and the optimum gains remain effective despite significant changes in load and system parameters. The control scheme's performance is also assessed under random step load disturbances. This study focuses on regulating the frequency of a microgrid in island mode across various scenarios. An objective function based on time and frequency fluctuations is defined, with PID controller parameters transformed into an optimization problem solved by the hybrid PSO-GSA algorithm. Four scenarios are examined: (a) dynamic microgrid model and optimal PID coefficients; (b) system disturbance with varying

velocity to observe power and frequency changes; (c) stepped load variations; and (d) application of the proposed methods to a standard test function. Simulations show that the proposed control method improves microgrid frequency stability under diverse operating conditions [3]. In Article [4]the Load Frequency Control (LFC) of a multi-source microgrid, which includes renewable energy sources. To ensure a consistent power supply, the system's frequency must be kept stable. The article presents a PID controller as a secondary controller to maintain the microgrid's frequency during the island mode. The performance index used is the integral of squared time multiplied by error squared (ISTES). Craziness-Based Particle Swarm Optimization (CRPSO) is proposed as an improved version of Particle Swarm Optimization (PSO) to optimize the nonlinear problem of load and frequency controller design, which improves the convergence speed. This paper proposes a fuzzy-based frequency control method for a PV generator in a PV-diesel hybrid system, addressing power fluctuations without smoothing the PV output. The method achieves effective power control by considering utility conditions and maximizing energy capture, thereby mitigating frequency deviations in the grid caused by large PV penetration [7].

The performance of Load Frequency Control (LFC) for isolated power systems with thermal, hydro, and gas power-generating units is studied using a Proportional-Integral-Derivative (PID) controller. The PID controller is implemented as a subordinate controller to stabilize the system during sudden power demand changes. Optimal gain values for the PID controller are obtained using the Particle Swarm Optimization (PSO) algorithm. Cost functions such as Integral Time Absolute Error (ITAE), Integral Absolute Error (IAE), Integral Squared Error (ISE), and Integral Time Squared Error (ITSE) are used for optimization. The PSO-based PID controller is compared with conventional, Differential Evolution (DE), and Genetic Algorithm (GA) based PID controllers, showing faster response settling and improved performance [8] The primary objective of this research is to analyze the frequency response of a two-area interconnected power system under load increments and variations in photovoltaic (PV) generation using a PSO-based PID controller. Additionally, the study aims to evaluate the robustness and adaptability of the proposed controller under diverse operating conditions.

2. Methodology

The proposed methodology involves the modeling of a two-area power system, considering the interaction between generation and load. Area 1 consists of a hydropower system and a photovoltaic (PV) system, while Area 2 is solely composed of a hydropower system. For both areas, and the tie-line, PID controllers are employed to manage the dynamics of the system. The study investigates three distinct cases:

- Case 1: An increase in load by 0.2 p.u in both areas.
- Case 2: An increase in load by 0.4 p.u in both areas.
- Case 3: An increase in load by 0.5 p.u in both areas.

The system's performance under these conditions is analyzed using two methods: the conventional Ziegler-Nichols method and the Particle Swarm Optimization (PSO) method. Subsequently, PSO is applied to optimize the parameters of the PID controllers. The effectiveness of the PSO-optimized PID controller is then analyzed and compared across the aforementioned load conditions, providing insights into the potential improvements in system stability and performance. The computer specifications used in this article include Microsoft Windows 11 Pro as the operating system and an AMD Ryzen 7 7730U processor with

Radeon Graphics, operating at 2.00 GHz with 8 cores. It is a 64-bit system with an x64-based processor. The device offers 512 GB of storage and 8 GB of RAM. The software utilized is MATLAB R2022b, and the optimization tools employed are Particle Swarm Optimization and the Ziegler–Nichols method.The overall methodology of the research is shown in figure 1.

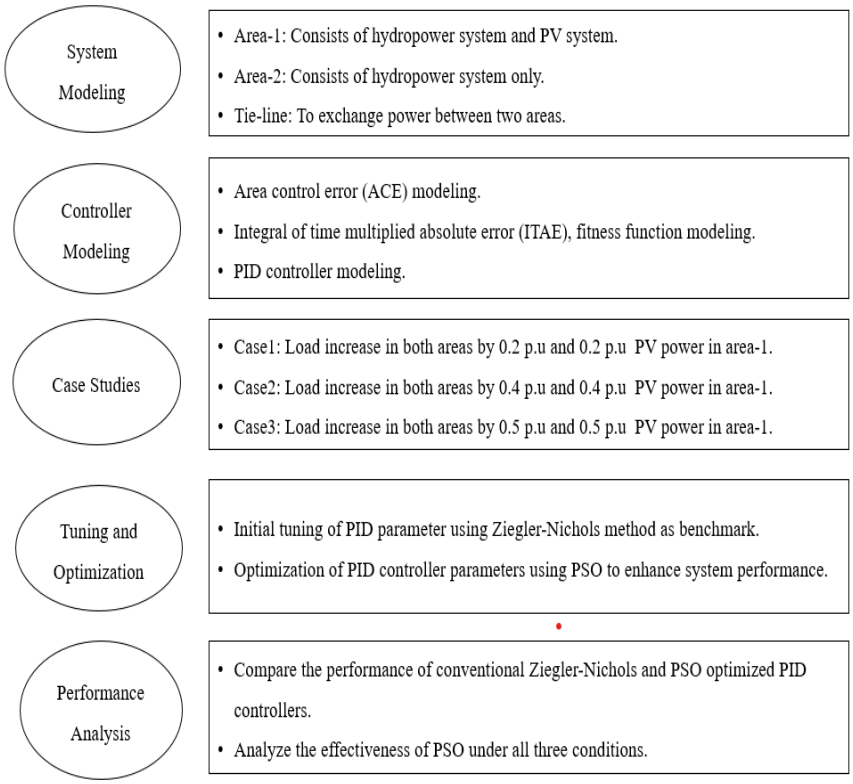

Figure 1: Overall Methodology for the research study

2.1 Modeling of Components

The mathematical modeling of a two-area power system includes the speed governor model, turbine model, generator load model, tie-line model, and PV model.

2.1.1 Governor Model

The speed governor model can be formulated by analyzing several steady-state conditions [9]. Assuming a linear relationship and considering a single time constant T_g, we have the following domain relations and equations are represented by equation 1and 2.

$$\Delta P_g(s) = \Delta P_{ref}(s) - \frac{1}{R}\Delta w(s) \quad (1)$$

$$\Delta P_v(s) = \frac{1}{1+sT_g}\Delta P_g(s) \quad (2)$$

The resulting speed governor model is shown in Figure 2 , where, R = Speed regulation of the governor and T_g= time constant of a speed governor.

2.1.2 Turbine Model

The model for the turbine relates changes in the mechanical power output ΔP_m to changes in valve position ΔP_v [9].The simplest turbine model can be approximated as by equation 3.

$$G_T(s) = \frac{\Delta P_m(s)}{\Delta P_v(s)} = \frac{1}{1+T_T(s)} \quad (3)$$

The block diagram of the simple turbine is shown in Figure 3.

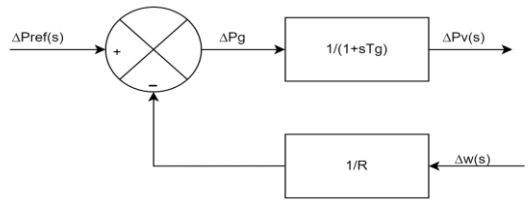

Figure 2: Block diagram of speed governor model

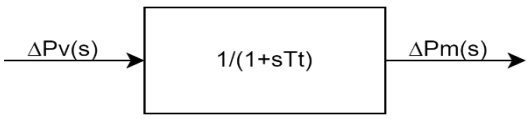

Figure 3: Block diagram of Turbine Model

2.1.3 Generator Load Model

The load on the power system consists of a variety of electrical devices. For resistive loads, such as lighting and heating loads, the electrical power is independent of frequency. Motor loads are sensitive to changes in frequency [9]. How sensitive it is to frequency depends on the composite of speed load characteristics of all the driven devices. The speed-load characteristics of a composite load are approximated by equation 4.

$$\Delta P_e = \Delta P_L + D\Delta w \quad (4)$$

where, ΔP_L is the non-frequency sensitive load change, and DΔw is the frequency sensitive load change. D is expressed as a percentage change in load divided by a percentage change in frequency. The block diagram representation of the generator-load model is shown in Figure 4.

2.1.4 Tie- line Model

In an interconnected power system, areas are connected by tie lines for power-sharing. If the frequency in each control area remains within the preset value, no power flow is needed through the tie lines. However, if there is a power imbalance in one area, power flows through the tie lines to another area to balance the load and maintain frequency within acceptable limits. The Laplace transformation of the tie line is given in equation 5 and tie-line model in Figure 5.

$$\Delta P_{tie} = \frac{2\pi T_{ij}}{s}(\Delta f_I - \Delta f_j) \quad (5)$$

Where, j=2 as i=1 and j=1 as i=2.

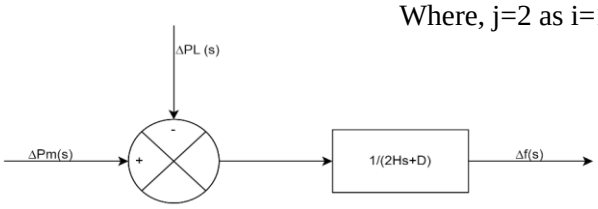

Figure 4: Generator load model

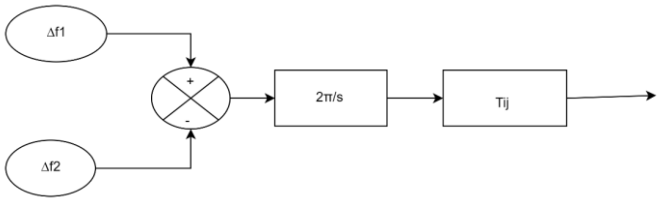

Figure 5: Tie-line model

2.1.5 PV Model

The photovoltaic (PV) model converts sunlight into electrical energy directly. It consists of a combination of PV cells connected in series and parallel. The performance of the PV system is primarily influenced by factors such as solar irradiance, ambient temperature, the tilt angle of the solar panels, and shading on the panels. The power generated by PV array is given by equation 6.

$$P_{pv} = \eta s \phi\,(1\text{-}0.005\,(T_a + 25)) \quad (6)$$

where, η is the conversion efficiency of the PV array (%), ϕ is solar radiance, S is measured area of PV array (m^2), and T_a is ambient temperature [5]. It is an intermittent source of

energy, and intermittency involved with solar power is taken as 5%. The simplified transfer function used for PV power generation system is defined in equation 7.

$$G_{PV}(s) = \frac{K_{pv}}{1+ST_{pv}} = \frac{\Delta P_v}{\Delta \phi} \quad (7)$$

where, K_{pv} and T_{pv} represent the gain and time constant of PV panel respectively.

2.1.6 Inverter Model

A solar power system generates DC power, but most electrical loads operate on AC power. Therefore, it's necessary to convert the DC power to AC using an appropriately sized inverter. The mathematical modeling of an inverter can be expressed using a transfer function, which describes the system's behavior in terms of input and output relationships as shown in equation 8.

$$G_{pI}(s) = \frac{K_{pi}}{1+ST_{pi}} \quad (8)$$

2.2 PID Controller

PID controllers are widely used in industrial processes due to their fast, efficient control, simple structure, ease of application, and robust performance. However, determining the three controller parameters (Kp, Ki, Kd) during the design phase, known as the "tuning process," is challenging and crucial to success. Advanced tuning methods, like model-based techniques, have been developed to enhance controller performance. The proportional controller gives an output that is proportional to the error signal. Due to the limitation of the P-controller where there always exists an offset between the process variable and set-point, the I-controller is needed which provides the necessary action to eliminate the steady-state error. It integrates the error over a period of time until the error values reach zero. But, it limits the speed of response and affects the stability of the system. Derivative gain controller can predict the future behavior of the error. Its output depends on the rate of change of error with respect to time, multiplied by the derivative constant. It reduces overshoot and speeds up output but increases steady-state error.

2.3 PID Controller Structure

To maintain the scheduled system frequency and scheduled tie-line power, PID controllers are implemented in both areas of the two-area systems being analyzed. The Area Control Error (ACE) is defined by equation 9. The control input signal U, is provided to the respective control area. PID controller structure is shown in Figure 6.

$$U = K_{pi} ACE_i + K_i \int_0^t ACE_i(t)\, d(t) + K_{Di} \frac{ACE(t)}{dt} \quad (9)$$

where K_p, K_i and K_d are proportional, integral, and derivative gains of the controller.

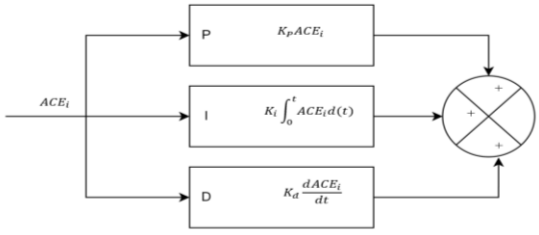

Figure 6: PID controller structure

2.4 Ziegler-Nicholas Tuning Method

The Ziegler–Nichols method is a popular technique for tuning P, PI, and PID controllers. It involves setting the integral and derivative gains to zero and gradually increasing the proportional gain until the system displays sustained oscillations. The value of the proportional gain at which the system first exhibits these oscillations is called the critical gain (Kcr), which is determined experimentally. The corresponding value of the proportional period (Pcr) can be obtained using MATLAB Simulink. If the system fails to exhibit sustained oscillations regardless of the proportional gain value, this method cannot be applied. A flowchart for the Ziegler–Nichols method is illustrated in Figure 7.

The P, I, and D gains are set according to Table 1.

Table 1: PID Gains according to Ziegler–Nichols Method

Controllers	K_p	T_I	T_D
P	$0.5k_{cr}$	∞	0
PI	$0.45k_{cr}$	$\frac{1}{1.2}P_{cr}$	0
PID	$0.6k_{cr}$	$0.5P_{cr}$	$0.125P_{cr}$

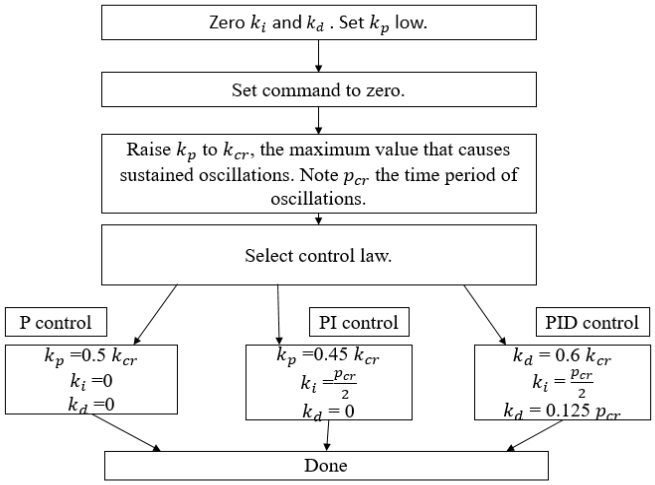

Figure 7: Flow chart for the Ziegler-Nichlos method

2.5 PSO Algorithm

Particle Swarm Optimization (PSO) is an iterative computational technique inspired by the social behavior of fish and birds. It optimizes a candidate solution by having particles, initially placed randomly, search for the minimum value in a solution space. Each particle moves towards both its personal best position and the global best found by the swarm. The algorithm continues refining the solution through successive iterations, with particles adjusting their positions and velocities to approach the target. The velocity and position of the i_{th} particle are determined through equations 10 and 11.

$$v_i^{(t+1)} = w * v_i^{(t)} + c_1 * r_1(Pbest_i - X_i) + c_2 r_2(gbest - x_i) \quad (10)$$

$$x_i^{(t+1)} = x_i^{(t)} + v_i^{(t+1)} \quad (11)$$

where,

$v_i^{(t+1)}$ = velocity of the particle at $(t+1)^{th}$ iteration; w = Inertia weight; v_i^{th} = velocity at t^{th} iteration ; c_1, c_2 = acceleration coefficients; x_i^{th} = position of the particle at t^{th}iteration

$x_i^{(t+1)}$ = position of the particle at $(t+1)^{th}$ iteration, $r_1 r_2$ is random function; g_{best} = global best of the particles

In Particle Swarm Optimization (PSO), acceleration coefficients, denoted as c_1 and c_2, control the balance between exploration and exploitation. The cognitive component, c_1, guides a particle towards its own best position, emphasizing exploitation of individual experience. The social component, c_2, directs the particle towards the swarm's best position, encouraging exploration. Higher $c_1$values prioritize exploitation, while higher c_2 values favor exploration. These coefficients are critical in determining convergence speed and solution quality, typically set around 2. Additionally, random functions, usually generating values between 0 and 1, initialize particle positions and velocities. The parameter setting of the PSO is shown in Table 2.

Table 2: Parameter setting of the PSO

Number of variables	9
Number of particles	15
Number of iterations	100
Upper bound of variables(u_b)	1
Lower bound of variables(l_b)	-1
Maximum inertia weight (w_{max})	1
Minimum inertia weight (w_{min})	0.1
Personal acceleration coefficient (c_1)	2
Global acceleration coefficient (c_2)	2

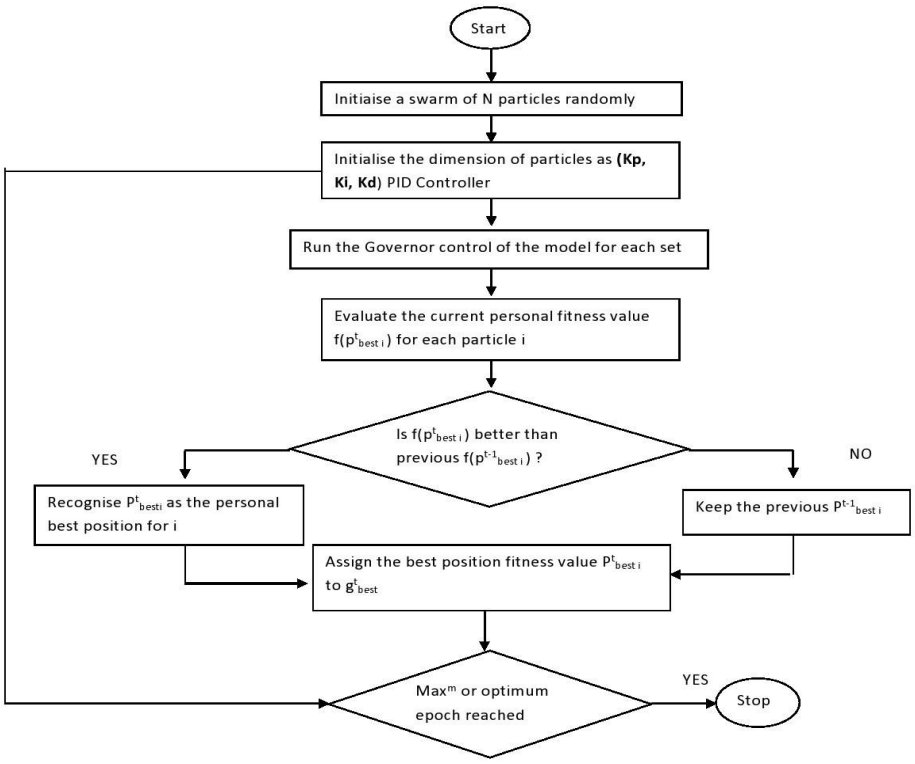

Figure 8: Flowchart of PSO based PID algorithm

The flowchart [10] of PSO based PID algorithm is shown in Figure 8.

2.6 Area Control Error

Area Control Error (ACE) measures the difference between scheduled or desired frequency and actual frequency in control areas. It serves as a feedback signal in the control system, adjusting generation and load to maintain system frequency within acceptable limits. Conventional Load Frequency Control (LFC) focuses on tie-line control, aiming to reduce ACE to zero in each area. The control error for each area consists of a linear combination of frequency and tie-line error [9]. Equation to represent area control area is given below.

$$ACE_i = \int_{j=1,\dots,n,}^{n} \Delta P_{ij} + K_i \Delta f_I \quad (12)$$

where,

ACE is the area control error for a specific control area.

Δf is the frequency deviation for that area. It represents the difference between the scheduled (reference) frequency and the actual frequency in each control area. Mathematically, it can be expressed as:

Δf = f-reference – f-actual

ΔP represents the difference between the scheduled tie-line power flow and the actual tie-line power flow between the two control areas. Mathematically, it can be expressed as:

ΔP = P-scheduled – P-actual

The area bias K_i influences the level of interaction during disturbances in adjacent areas. Optimal efficiency is achieved when K_i is set equal to the frequency factor of the respective area [9]. The frequency response characteristic of the area is given by equation 13.

$$B_i = \frac{1}{R_i} + D_i \quad (13)$$

Thus, the ACEs for a two-area system are.

$$ACE_1 = \Delta P_{12} + B_1 \Delta f_1 \quad (14)$$

$$ACE_2 = \Delta P_{21} + B_2 \Delta f_2 \quad (15)$$

Here, ΔP_{12} *and* ΔP_{21} represent departures from the scheduled interchange. ACEs are used as actuating signals to activate changes in the reference power-set points, and when the steady-state is reached ΔP_{12} and Δw will be zero. The integrator gain constant must be chosen small enough so as not to cause the area to go into a chase mode.

2.7 Control Structure

A system is considered an optimal control system when the controller parameters are adjusted to minimize the objective function. In the design of a Particle Swarm Optimization (PSO) algorithm for optimizing a PID controller, the objective function is first defined based on the desired specifications and constraints. The objective function for tuning PID controller parameters typically relies on performance indices that evaluate the entire closed-loop response. For Load Frequency Control (LFC) design, some of the key specifications include:

- Frequency deviations and tie-line power deviations should return to zero as quickly as possible following a step load change.

- The integral of frequency deviations and tie-line power deviations should be minimized.

To satisfy these specifications, [12], [13] conventional performance indices such as the Integral of Time multiplied Absolute Error (ITAE) is used as minimization function as shown in equation 16.

$$ITAE = \int_0^t (|\Delta f_1| + |\Delta f_2| + |\Delta P_{tie}|) \cdot t \cdot dt \quad (16)$$

In the above formulas, $\Delta f1$ and $\Delta f2$ are the frequency deviation of the control area first and second respectively. $\Delta Ptie$ is the tie line power deviation. t is the maximum simulation time [12]. The goal of PSO is to find the particle whose position minimizes the ITAE value, which corresponds to the global best solution.

2.9 Modeling of two area interconnected power system.

The block diagram model of a two-area interconnected power system with a PSO-based PID controller is shown in Figure 9. The state equations for the two-area interconnected power system are derived using the transfer function. From the block diagram model, it is clearly seen that there are two control input U_1 and U_2. ΔP_{tie} is a tie-line power change and Δf_1 and Δf_2 are frequency deviation. The block diagram represents an interconnected power system with two areas linked by a tie line. Both areas use hydropower systems, consisting of governors, turbines, and generators. PID controllers are employed in Area-1, Area-2, and the tie line. To minimize the rise time, overshoot, settling time, and steady-state error, the proposed method utilizes the PSO algorithm to optimize the controller gain values of K_p, K_i and K_d. These values are attained by MATLAB simulation.

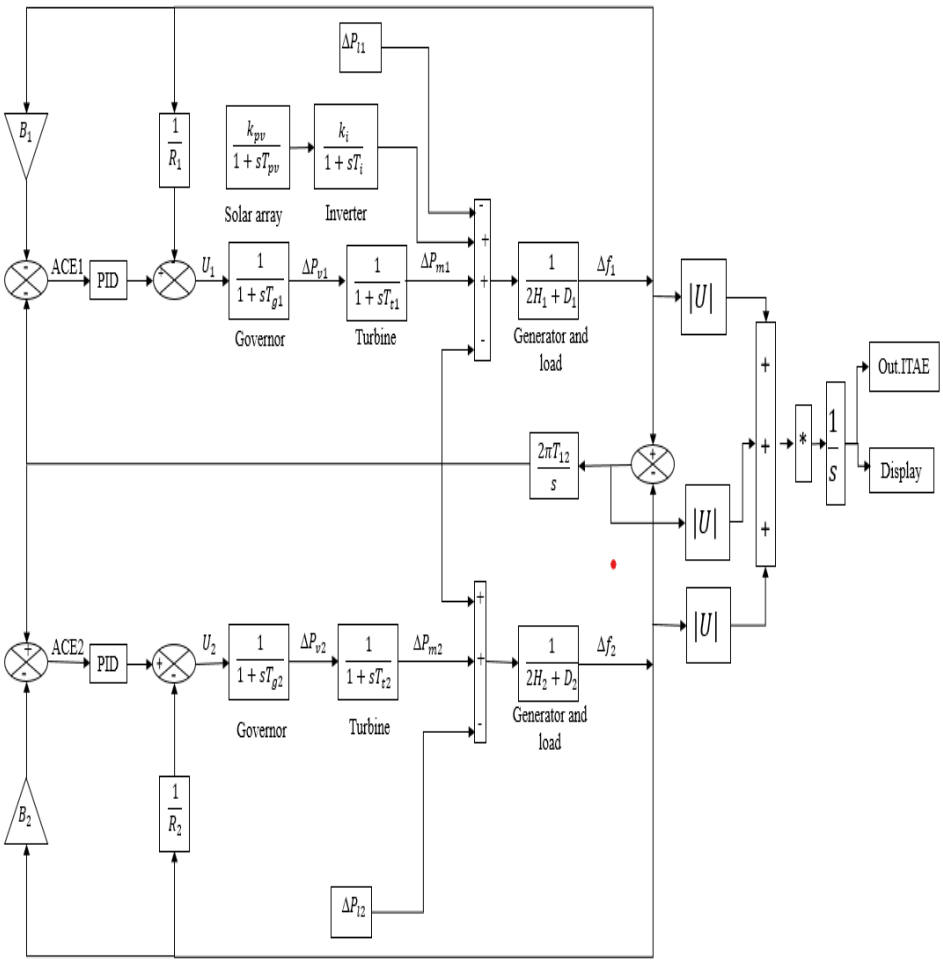

Figure 9: State-space model of two area system

3. Results and Discussions

The Simulink model for frequency control was developed using the transfer functions of a power network in MATLAB/Simulink. A PID controller was optimized using Particle Swarm Optimization (PSO) with an ITAE-based objective function. Nominal system parameters are provided in Appendix A. The load frequency control of a two-area power system was simulated, considering load and solar generation variations. Frequency deviations in both areas were analyzed with Ziegler-Nichols (Z-N) and PSO-based PID controllers. The three cases of load and solar generation variations (0.2, 0.4, and 0.5 p.u) were tested. The results demonstrate the effectiveness of the proposed PSO-based strategy for load frequency management.

3.1 Load increment of 0.2 p.u in both area and solar output of 0.2 p.u in area-1.

At t =2sec, a 0.2 p.u. solar output is introduced in Area-1, and at t =20 sec, a 0.2 p.u. step load increase occurs in both areas. The resulting frequency disturbances in both areas, caused by changes in load and generation, are depicted in the figure 10. The dynamic response of the system, achieved using a PID controller with Z-N and PSO tuning methods, is also shown in figure 11. The PSO optimization technique significantly reduces frequency deviation, with noticeable improvements in settling time and undershoot in both areas.

The impact is more pronounced in Area-1 due to solar generation but is evident in Area-2 as well. Both PSO and Z-N methods effectively limit frequency deviations within 2% in this case.

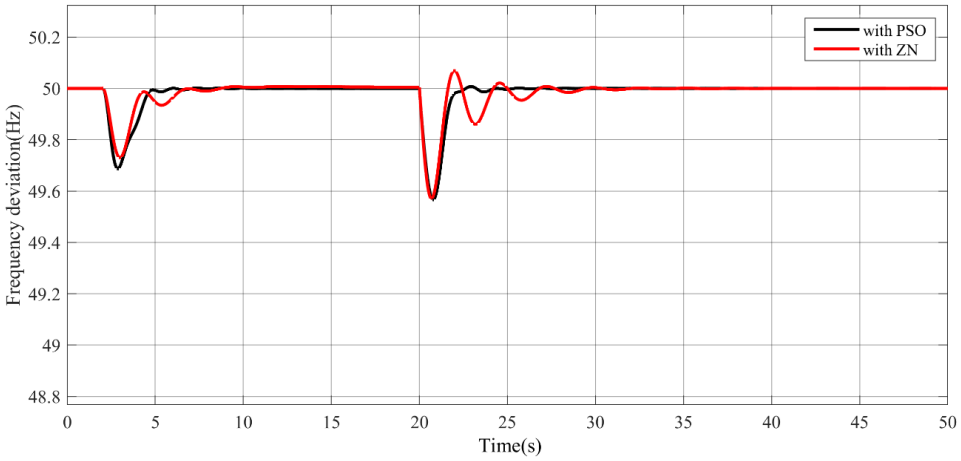

Figure 10: Frequency deviation in area-1 for 0.2 p.u step load change in both area and solar output of 0.2 p.u in area-1

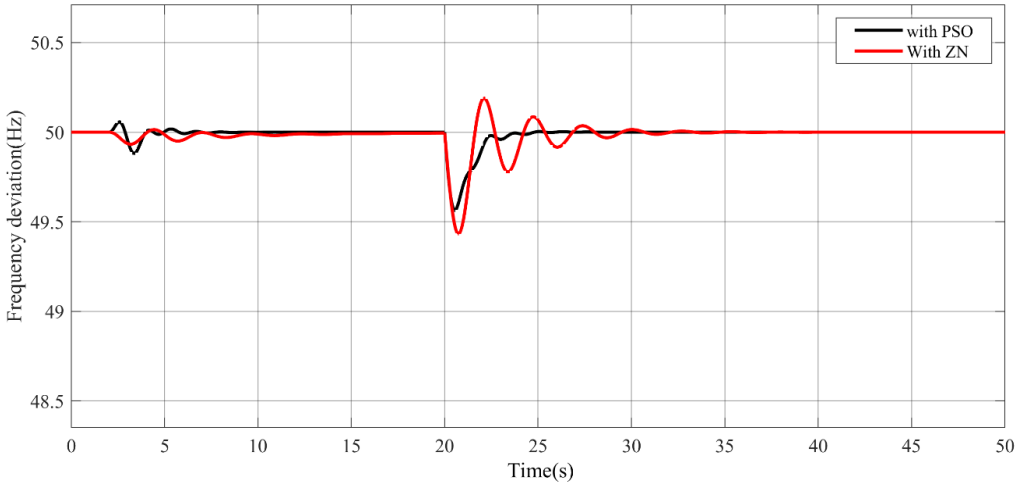

Figure 11: Frequency deviation in area-2 for 0.2 p.u step load change in both area and solar output of 0.2 p.u in area-1

3.2 Load increment of 0.4 p.u in both area and solar output of 0.4 p.u in area-1

At t=20 sec, a step load increase of 0.4 p.u. was applied in both areas. Additionally, at t =2sec, a 0.4 p.u solar power output was introduced in Area-1. The dynamic response obtained using the PID controller, tuned through Ziegler-Nichols (Z-N) and Particle Swarm Optimization (PSO), is presented in the Figure 12. The frequency disturbances resulting from the changes in load and generation are also depicted in the Figure 13. The settling time and undershoot has been drastically reduced using PSO optimization rather than Z-N technique. In area-1 both optimization technique are capable to limits frequency above 49 Hz, but in area-2 PSO is able to keep frequency above 49 Hz but Z-N cannot do so. Also effect of solar output is also more evident as solar output power of 0.4 p.u is obtain from area-1.

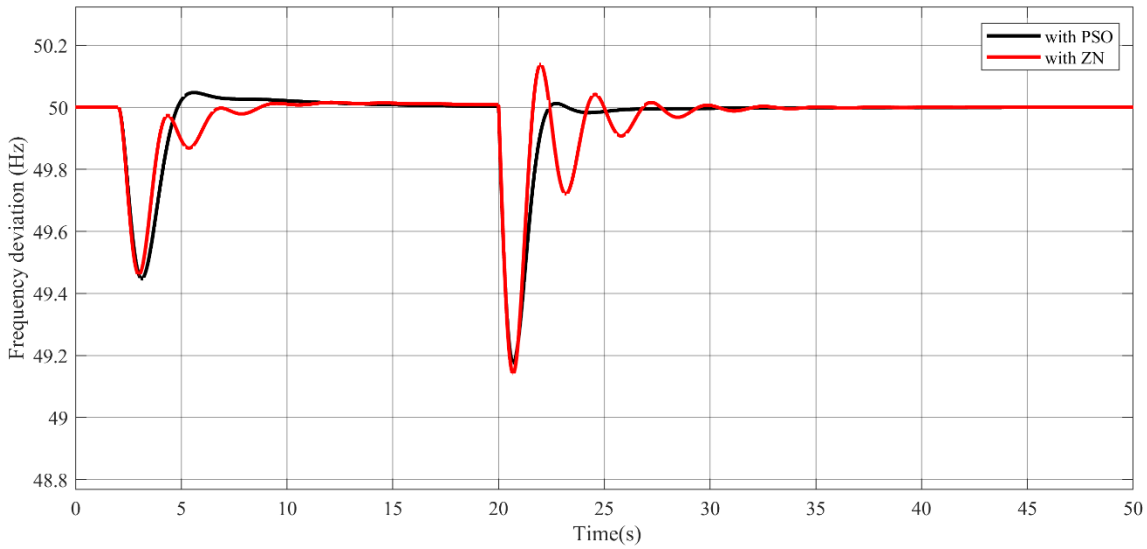

Figure 12: Frequency deviation in area-1 for 0.4 p.u step load change in both area and 0.4 solar output in area-1

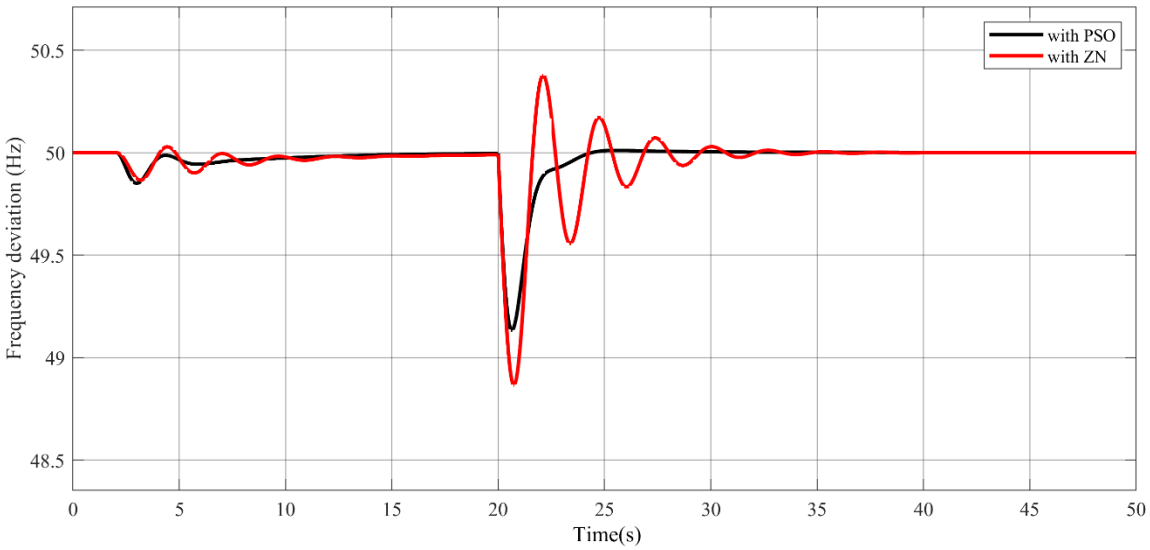

Figure 13: Frequency deviation in area-2 for 0.4 p.u step load change in both area and solar output of 0.4 p.u in area-1.

3.3 Load increment of 0.5 p.u in both area and solar output of 0.5 p.u in area-1

A 0.5 p.u. step load increase was applied to both areas at t = 20 seconds, while a 0.5 p.u. solar output was introduced in area-1 at t =2 seconds. The dynamic response obtained using a PID controller tuned with the Ziegler-Nichols (Z-N) method and Particle Swarm Optimization (PSO) is illustrated in the Figure 14. The frequency disturbances in both areas resulting from the changes in load and generation are also depicted in the Figure 15.

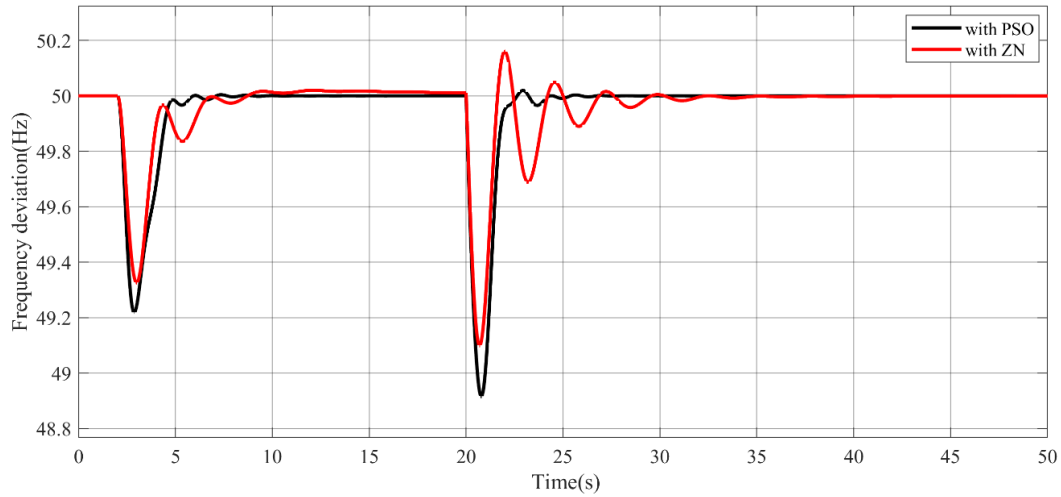

Figure 14: Frequency deviation in area-1 for 0.5 p.u step load increment in both area and 0.5 p.u solar output in area-1

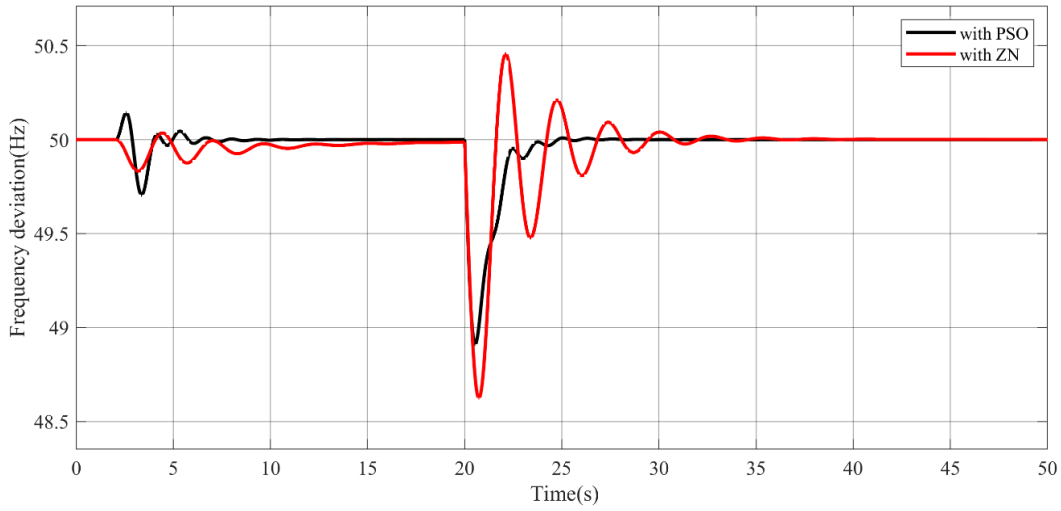

Figure 15: Frequency deviation in area-2 for 0.5 p.u step load increment in both area and 0.5 p.u solar output in area-1

The applied technique effectively improved both settling time and undershoot. In Area-1, the frequency remains within acceptable limits while using PSO. However, without PSO, the frequency drops below the 49 Hz threshold, violating the limit. In Area-2, neither of the applied methods can maintain the frequency within the permissible range. It is also important to note that if the load change increases to approximately 50% of the generation in both areas, the frequency limit is violated even with PSO. Additionally, as the output from the solar array increases, the frequency deviation becomes more pronounced. Therefore, there is a limit to the amount of solar penetration that the system can accommodate.

3.4 Parameter setting of PID controller

The optimized parameter setting of PID controller obtained using Z-N method and PSO is shown in Table 3.

Table 3: Parameter settings of PID controller

Method of optimization	Area-1			Area-2			Area-3		
	K_P	K_I	K_D	K_P	K_I	K_D	K_P	K_I	K_D
With ZN	1.26	0.841	0.2971	1.2	0.868	0.287	1.23	0.6718	0.3721
With PSO	0.5982	1	0.4613	0.9992	1	0.9859	1	-0.000001	-0.8142

`3.5 Convergence of objective function

The convergence analysis demonstrates the effectiveness of the PSO algorithm in minimizing the ITAE objective function. Throughout the iterative process, the ITAE value progressively decreases, with the global best solution stabilizing as the algorithm converges. This behavior underscores the reliability of PSO in achieving optimal solutions for control system optimization. The results validate both the selection of ITAE as the objective function and the efficacy of PSO as an optimization tool. In the first iteration, the global best ITAE value is 30.5019. By the second iteration, it rapidly decreases to approximately 1.8086, attributed to extensive exploration of the search space. In the intermediate phase, gradual improvements are observed as particles refine their positions toward better solutions. Finally, in the convergence phase, the ITAE value stabilizes, indicating the algorithm's successful attainment of an optimal solution. By the 100th iteration, the ITAE value reaches 0.01362.

The convergence graph of the ITAE objective function using the PSO algorithm is presented in Figure 16.

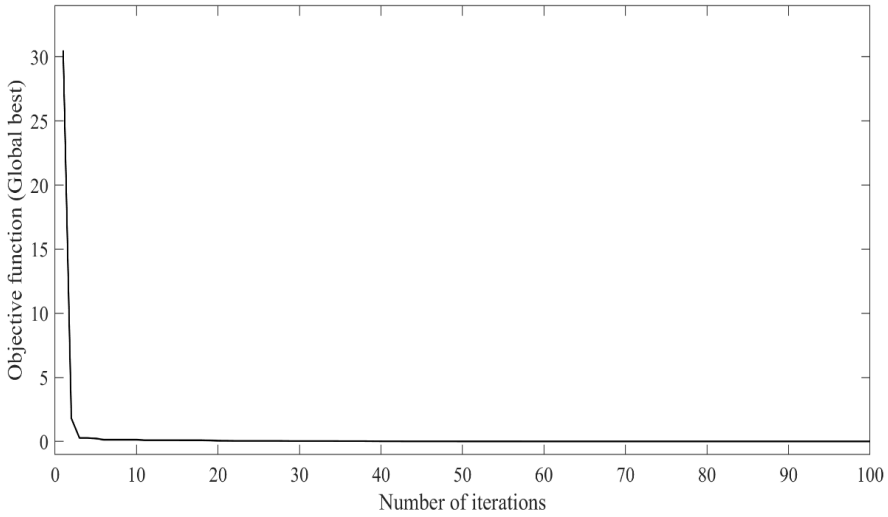

Figure 16: Convergence graph of ITAE function

3.6 Limitations

The study has several key limitations. It uses a simplified two-area power system model, which excludes the complexities of real-world systems, such as interconnected areas, nonlinearities, and dynamic factors. The integration of the solar PV system in Area-1 assumes static output characteristics, neglecting factors like rapid variations in solar

irradiance, temperature effects, and inverter dynamics. The focus on a linear PID controller overlooks the potential benefits of nonlinear or adaptive control techniques, which could perform better under uncertain or nonlinear conditions. While Particle Swarm Optimization (PSO) is effective for optimizing PID gains, its computational complexity may increase with larger or higher-dimensional systems, limiting real-time applicability. Additionally, the study is limited to frequency control, excluding other important aspects of power system stability, such as voltage regulation and transient stability.

4. Conclusions

The study of the LFC for a Two-area interconnected power system with a PSO-based PID controller was presented in this work. The power system consists of hydropower and solar PV in area-1, and hydropower in area-2. Gain settings for PID controller were estimated using PSO algorithm. The optimal value of the proposed PSO-based PID controller parameters is obtained by minimizing the ITAE objective function. Three cases, case 1: an increase in load both area and solar output of 0.2 p.u, case 2: an increase in load in both areas and solar output of 0.4 p.u, and case 3: an increment of load in both area and solar output of 0.5 p.u were considered for study. The outputs of frequency in area-1and frequency in area-2 of the system were plotted with conventional Z-N method and with PSO. It was found that in all cases, PSO has significantly reduced frequency deviation. Settling time, overshoot, and undershoot are also reduced by the PSO-based PID controller. Therefore, it can be concluded that the proposed controller can enhance power system operation, and stability by reducing frequency deviation. The robustness and adaptability of the proposed controller under various operating conditions are satisfied.

Conflicts of Interest Statement

The authors declare no conflicts of interest for this study.

Data Availability Statement

The data that support the findings of this study are available from the corresponding author upon reasonable request.

References

1. M. Basukala, N. Regmi, and S. Gurung, “Proceedings of 12 th IOE Graduate Conference Load Frequency Control of Integrated Nepal Power System.”
2. S. Poudel and A. Singh, “Genetic Algorithm-based PID Controller for Load-Frequency Control in Two Area Interconnected Power System.”
3. F. Zishan, E. Akbari, O. D. Montoya, D. A. Giral-Ramírez, and A. Molina-Cabrera, “Efficient PID Control Design for Frequency Regulation in an Independent Microgrid Based on the Hybrid PSO-GSA Algorithm,” *Electronics (Switzerland)*, vol. 11, no. 23, Dec. 2022, doi: 10.3390/electronics11233886.
4. R. Alayi, F. Zishan, S. R. Seyednouri, R. Kumar, M. H. Ahmadi, and M. Sharifpur, “Optimal load frequency control of island microgrids via a PID controller in the presence of wind turbine and PV,” *Sustainability (Switzerland)*, vol. 13, no. 19, Oct. 2021, doi: 10.3390/su131910728.
5. A. Dutta and S. Prakash, “Load frequency control of multi-area hybrid power system integrated with renewable energy sources utilizing FACTS & energy storage system,” *Environ Prog Sustain Energy*, vol. 39, no. 2, Mar. 2020, doi: 10.1002/ep.13329.

6. B. Prakash Ayyappan, U. Thiruppathi, and G. Balaganapathi, "Load Frequency Control of an Interconnected Power System Using Thyristor Controlled Phase Shifter (TCPS)." [Online]. Available: www.ijert.org
7. M. Datta, T. Senjyu, A. Yona, T. Funabashi, and C. H. Kim, "A frequency-control approach by photovoltaic generator in a PV-diesel hybrid power system," *IEEE Transactions on Energy Conversion*, vol. 26, no. 2, pp. 559–571, Jun. 2011, doi: 10.1109/TEC.2010.2089688.
8. J. M. Pearce *et al.*, "Load Frequency Control Assessment of a PSO-PID Controller for a Standalone Multi-Source Power System," 2023, doi: 10.3390/technologies.
9. "Power-System-Analysis-by-Hadi-Saadat-Electrical-Engineering-libre".
10. V. N. Ogar, S. Hussain, and K. A. A. Gamage, "Load Frequency Control Using the Particle Swarm Optimisation Algorithm and PID Controller for Effective Monitoring of Transmission Line," *Energies (Basel)*, vol. 16, no. 15, Aug. 2023, doi: 10.3390/en16155748.
11. A. M. Abdel-Hamed, A. Y. Abdelaziz, and A. El-Shahat, "Design of a 2DOF-PID Control Scheme for Frequency/Power Regulation in a Two-Area Power System Using Dragonfly Algorithm with Integral-Based Weighted Goal Objective," *Energies (Basel)*, vol. 16, no. 1, Jan. 2023, doi: 10.3390/en16010486.
12. G. Chen, Z. Li, Z. Zhang, and S. Li, "An Improved ACO Algorithm Optimized Fuzzy PID Controller for Load Frequency Control in Multi Area Interconnected Power Systems," *IEEE Access*, vol. 8, pp. 6429–6447, 2020, doi: 10.1109/ACCESS.2019.2960380.
13. M. Mokhtar, M. I. Marei, M. A. Sameh, and M. A. Attia, "An Adaptive Load Frequency Control for Power Systems with Renewable Energy Sources," *Energies (Basel)*, vol. 15, no. 2, Jan. 2022, doi: 10.3390/en15020573.

Appendix A: Parameters

Parameters of Two area interconnected power system

Base Power for Both areas	1000MVA
Governor Time constant for area-1 (g_{t1})	0.2sec
Governor Time constant for area-2 (g_{t2})	0.3sec
Turbine Time constant for area-1 (T_{t1})	0.5sec
Turbine Time constant for area-2 (T_{t2})	0.6sec
Inertia constant for area-1 (H_1)	$5m^2$/kg
Inertia constant for area-2 (H_2)	$4m^2$/kg
Frequency sensitive load coefficient for area-1 (D_1)	0.6
Frequency sensitive load coefficient for area-2 (D_2)	0.9
Speed regulation for area-1 (R_1)	0.05p.u/Hz
Speed regulation for area-2 (R_2)	0.0625p.u/Hz
Bias coefficient for area-1 (B_1)	20.6 MW/Hz
Bias coefficient for area-1 (B_2)	16.9 MW/Hz
Inverter parameters	K_i =1, T_i =0.4
Solar PV parameters	K_{pv}=1, T_{pv}=0.03

Appendix B: Simulink Layout